Electronic Supplementary Material (ESI) for CrystEngComm.

Electronic Supplementary Information

A phosphonate-lanthanoid polyoxometalate coordination polymer: $\{Ce_2P_2W_{16}O_{60}L_2\}_n$ zipper chains

Wenyan Wang,[a] Natalya V. Izarova,*[a,b] Jan van Leusen,[a] Paul Kögerler *[a,b]

[a] Institute of Inorganic Chemistry, RWTH Aachen University, D-52074 Aachen, Germany.

[b] Jülich-Aachen Research Alliance (JARA-FIT) and Peter Grünberg Institute 6, Forschungszentrum Jülich, D-52425 Jülich, Germany;

E-mails: paul.koegerler@ac.rwth-aachen.de; natalya.izarova@ac.rwth-aachen.de.

Experimental Details

Starting materials. The POT precursors $K_{10}[\alpha_2\text{-}P_2W_{17}O_{61}]\cdot 20H_2O$ (**K-{α_2-P_2W_{17}}**)[1] and $K_5H[\alpha_2\text{-}P_2W_{17}O_{61}(C_6H_5PO)_2]\cdot 4C_4H_9NO$ (**K-{α_2-P_2W_{17}(PhP)$_2$}**)[2] were prepared as previously reported and their identity was confirmed by IR spectroscopy. All other reagents were of analytical grade and were obtained from commercial sources and used without further purification.

Instruments. Elemental analyses (ICP-OES and C/H/N) were performed by Central Institute for Engineering, Electronics and Analytics (ZEA-3), Forschungszentrum Jülich GmbH (Jülich, Germany). Thermogravimetric/differential thermal analysis (TGA/DTA) measurements were carried out using a Mettler Toledo SDTA 851 in a dry N_2 flux (60 mL min^{-1}) at a heating rate of 5 K min^{-1}. FT-IR spectra were recorded on a Bruker Vertex 70 spectrometer using KBr pellets.

Diffuse reflectance spectra were recorded in the range of 300 − 800 nm on a UV-2600 Shimadzu UV-Vis spectrophotometer with $BaSO_4$ as a reference sample. For the measurement *ca*. 3 mg of **D-1** were dispersed on the surface of $BaSO_4$.

The magnetic data of **D-1** were collected using a Quantum Design MPMS-5XL SQUID magnetometer. The polycrystalline sample was compacted and immobilized into a cylindrical PTFE capsule. The data were recorded as a function of the magnetic field (0.1−5.0 T at 2.0 K) and the temperature (2–290 K at 0.1 T), and were corrected for the diamagnetic contributions of the sample holder and **D-1** ($\chi_{m,dia} = -1.43\times10^{-3}$ cm^3 mol^{-1}).

Synthesis of $[Ce^{III}(H_2O)_{4.5}]_{0.5}[(CH_3)_2NH_2]_{2.5}[(H_2O)_{9.25}Ce^{III}_2(\alpha_2,\alpha_2'\text{-}P_2W_{16}O_{60})(C_6H_5PO)_2]\cdot 17.5H_2O$ (D-1). A sample of **K-{α_2-P_2W_{17}(PhP)$_2$}** (0.050 g, 0.010 mmol) was added into a solution of $CeCl_3\cdot 7H_2O$ (0.011 g, 0.0295 mmol) in H_2O (10 mL). The reaction mixture was then stirred at room temperature for 4 hours under an opaque cover preventing light exposure. Subsequently, solid sample of dimethylamine

hydrochloride (DMACl; 0.025 g, 0.306 mmol) was added to the obtained solution under vigorous stirring. After that, the obtained mixture (pH 2.6) was filtered and the resulting light-green solution was left for evaporation in air, being protected from sun-light. Orange rhombic crystals of **D-1** were collected after two weeks. Yield: 0.032 g (67.7 % based on W).

We note that during the reaction and crystallization, the reaction solutions for preparation of orange rhombic plate-shaped crystals of **D-1** have to be protected from sunlight. This leads to the better yield and product purity as irradiation with the sunlight results in a partial reduction of W^{VI} centers of the POT moieties to W^{V} state as it is evident from the appearance of dark greenish-blue color of the reaction mixture. Furthermore any, even slight, heating of the reaction mixture has to be absolutely excluded as it enforces the release of the phenylphosphonate groups from $\{\alpha_2\text{-}P_2W_{17}(PhP)_2\}$ polyanions and to formation of Ce^{III} / $[\alpha_2\text{-}P_2W_{17}O_{61}]^{10-}$ complexes and non-lacunary Wells-Dawson polyanions $[\alpha\text{-}P_2W_{18}O_{62}]^{6-}$.

Elemental analysis, calculated for $C_{17}H_{88}Ce_{2.5}N_{2.5}O_{91}P_4W_{16}$, M_r = 5199.64 g/mol, (found): C, 3.93 (3.94); H, 1.71 (1.70); Ce, 6.74 (6.67); N, 0.67 (0.68); P, 2.38 (2.2); W, 56.57 (48.8) %. FT-IR (2 % KBr pellet), ν_{max} / cm^{-1}: 3420 (m, br); 1621 (w); 1463 (w); 1435 (w); 1384(m), 1155(m), 1133 (m); 1095 (m); 1064 (m);1024(m), 983(m), 941 (s); 844 (s); 773 (s); 696(s); 587 (s); 564 (s); 527 (s); 460(s).

Single-crystal X-ray diffraction data for **D-1** were collected at 100 K on a STOE STADIVARI diffractometer with MoKα radiation (λ = 0.71073 Å). A crystal was mounted in a Hampton cryoloop with Paratone-N oil to prevent water loss. Absorption corrections were applied by Gaussian integration using STOE X-Red32 software[3] and afterwards scaling of reflection intensities was performed within STOE LANA.[4] The SHELXTL software package[5] was used to solve and refine the structure. The structure was solved by direct methods and refined by full-matrix least-squares method against $|F|^2$ with anisotropic thermal parameters for all heavy atoms (Ce, P, W). The hydrogen atoms of the crystal waters and $–NH_2$ groups of the

dimethylammonium (DMA^+) countercation were not located, while the hydrogen atoms of the phenyl and methyl groups were placed in geometrically calculated positions. The crystal was refined as a 2-component inversion twin with a components ratio of 65.5 / 34.5 %.

The relative site occupancy factors for the disordered cerium atom (Ce3), solvent oxygens and DMA^+ cation were first refined in an isotropic approximation with U_{iso} = 0.05 and then fixed at the obtained values and refined without the thermal parameters' restrictions. Disordered positions of O26C / O27C were refined using a combination of PART / EAPD commands. Due to a severe disorder, we could not locate positions of all the dimethylammonium cations and co-crystallized water molecules. Thus, only one DMA^+ cation and 12 H_2O solvent molecules per formula unit could be unambiguously found from the X-ray diffraction data, while the presence of 2.5 DMA^+ ions and 17.5 crystal water molecules was established by elemental analysis. For overall consistency, the final formulae presented in the CIF files are based on the composition determined by a combination of single crystal X-ray (polyanion part) as well as elemental and thermogravimetric (exact number of cations and solvent molecules in the bulk material) analyses. The remaining electron density in the voids of the structures was treated by the SQUEEZE procedure.

Additional crystallographic data are summarized in Table S1. Further details on the crystal structure investigations can be obtained, free of charge, on application to CCDC, 12 Union Road, Cambridge CB2 1EZ, UK: http://www.ccdc.cam.ac.uk/, e-mail: data_request@ccdc.cam.ac.uk, or fax: +441223 336033 upon quoting CCDC 2070992.

Powder X-ray diffraction (PXRD) data (Figure S1) were recorded with a powder diffractometer (STOE STADI P). The experiments were performed on a flat sample in a transmission geometry using a Cu anode ($K\alpha_1$, λ = 1.54059 Å; 40 kV, 30 mA) and a focusing Johann-type Ge monochromator at room temperature. The omega angle was held at 55° and

the data were recorded with an image plate detector (140° in 2Θ, stepwidth 0.015°). The exposure times were between 3600 s.

For the measurements the crystals of **D-1** were grounded in the mother liquor (to prevent the removal of co-crystallized solvent molecules and a consequent loss of crystallinity) and placed into the sample holder together with a small amount of mother solution. We have found that the quality of mortaring (*i.e*. degree of the randomness of the crystals orientation in the sample holder) plays a crucial role for the quality of the obtained XRD patterns. However, due to the plate-like shape of the crystals even meticulous mortaring seemingly could not fully prevent a preferred orientation of the crystals in the employed sample. This is evident from the fact that despite the position of all the reflections in the simulated and experimental PXRD patterns match very well (confirming the phase purity of the powder material) there is a mismatch in their relative intensities, which indicates texturing of the sample.[6]

Table S1. Crystal data and structure refinement for **D-1**.

Empirical formula	$C_{17}H_{88}Ce_{2.5}N_{2.5}O_{91}P_4W_{16}$
Formula weight / g mol^{-1}	5199.67
Crystal system	Monoclinic
Space group	*C*2
a / Å	25.850(5)
b / Å	13.375(3)
c / Å	27.037(5)
β	91.89(3)°
Volume / Å^3	9343(3)
Z	4
D_{calc} / g cm^{-3}	3.697
Absorption coefficient / mm^{-1}	20.989
F(000)	9298
Crystal size / mm^3	0.05 × 0.28 × 0.30
Theta range for data collection	1.725° – 25.242°
Completeness to Θ_{max}	99.7%
Index ranges	$-31 \le h \le 30$, $-16 \le k \le 16$, $-32 \le l \le 32$
Reflections collected	120890
Independent reflections	17714
R_{int}	0.0828
Observed ($I > 2\sigma(I)$)	16927
Absorption correction	Gaussian integration

T_{min} / T_{max}	0.0276 / 0.1185
Data / restraints / parameters	17714 / 14 / 625
Goodness-of-fit on F^2	1.019
R_1, wR_2 ($I > 2\sigma(I)$)	R_1 = 0.0692, wR_2 = 0.1891
R_1, wR_2 (all data)	R_1 = 0.0708, wR_2 = 0.1919
Largest diff. peak and hole / e Å^{-3}	3.197 and –4.281

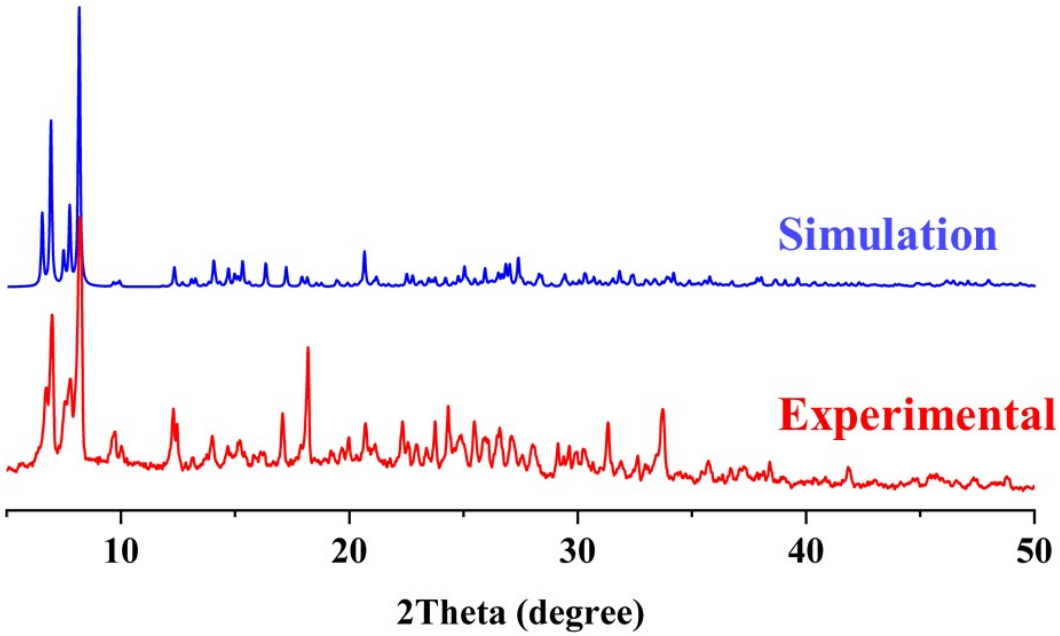

Figure S1. Experimental (red) powder X-ray diffraction pattern and simulated pattern based on the single-crystal XRD structure data (blue) for **D-1**.

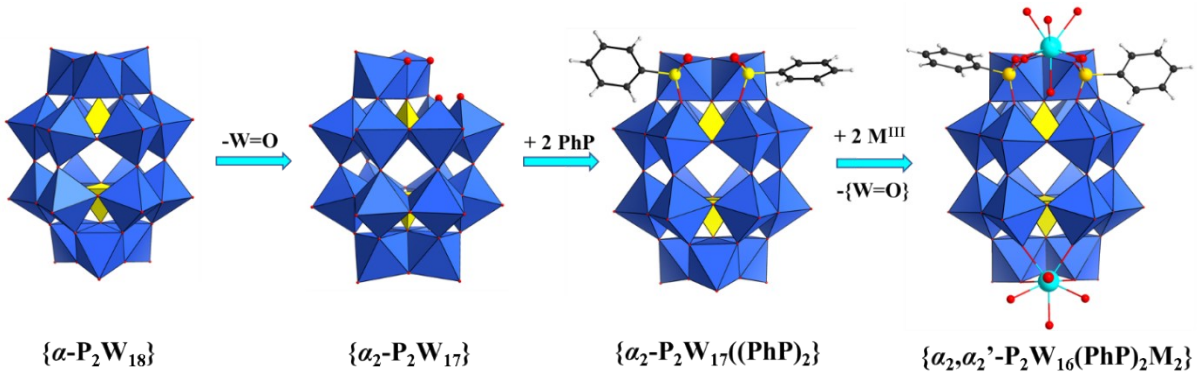

Figure S2. Structural interrelations between Wells-Dawson-type polyanion $[\alpha\text{-}P_2W_{18}O_{62}]^{6-}$ ($\{\alpha\text{-}P_2W_{18}\}$), its monolacunary derivative $[\alpha_2\text{-}P_2W_{17}O_{61}]^{10-}$ ($\{\alpha_2\text{-}P_2W_{17}\}$), phenylphosphonate-functionalized precursor $[\alpha_2\text{-}P_2W_{17}O_{61}(C_6H_5PO)_2]^{6-}$ ($\{\alpha_2\text{-}P_2W_{17}(PhP)_2\}$) and the monomeric unit $\{(H_2O)_{9.25}Ce^{III}_2(\alpha_2,\alpha_2'\text{-}P_2W_{16}O_{60})(C_6H_5PO)_2\}^{4-}$ ($\{\alpha_2,\alpha_2'\text{-}P_2W_{16}(PhP)_2M_2\}$) observed in the structure of **D-1**. Color code: $\{PO_4\}$: yellow tetrahedra, $\{WO_6\}$: blue octahedra; P: yellow, M: cyan-blue, O: red, C: black, H: white spheres.

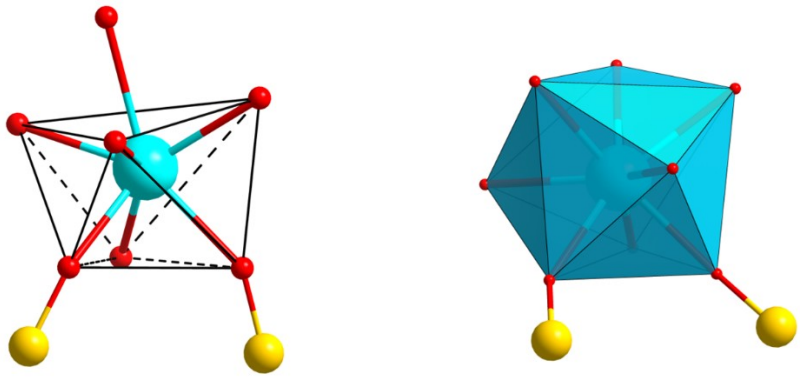

Figure S3. Coordination environment of the Ce_A^{III} center with coordination numbers 7 (25 % of polyanions) and 8 (75 % of polyanions)/

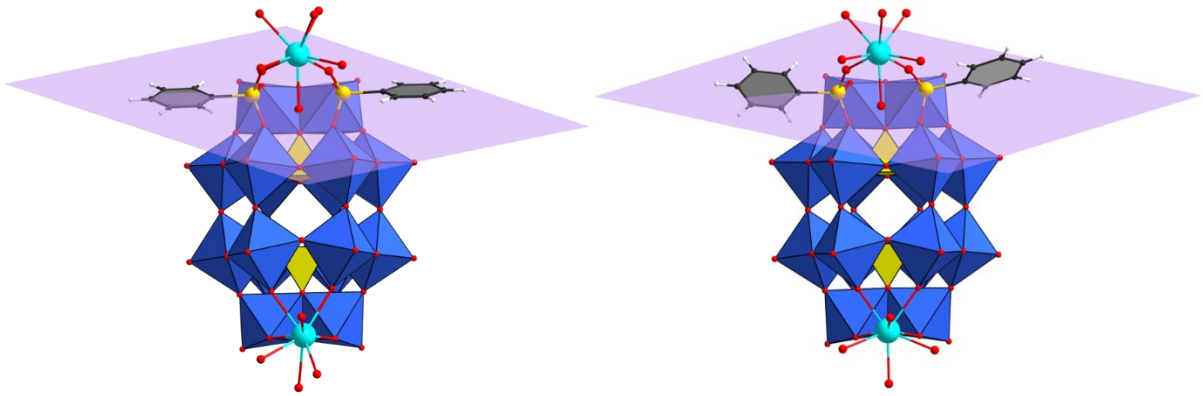

Figure S4. Comparison of mutual orientation of the phenyl rings in the monomeric units $\{(H_2O)_{9.25}Ce^{III}_2(\alpha_2,\alpha_2'\text{-}P_2W_{16}O_{60})(C_6H_5PO)_2\}^{4-}$ in **D-1** and $\{(H_2O)_7Dy^{III}_2(\alpha_2,\alpha_2'\text{-}P_2W_{16}O_{60})(PhPO)_2\}^{4-}$ in **CsK-2**. The planes are drawn through the P^V centers of phenylphosphonate groups and the O atoms of the $\{W_2\}$ "cap" that are bound to those P sites. Color code as in Figure S2.

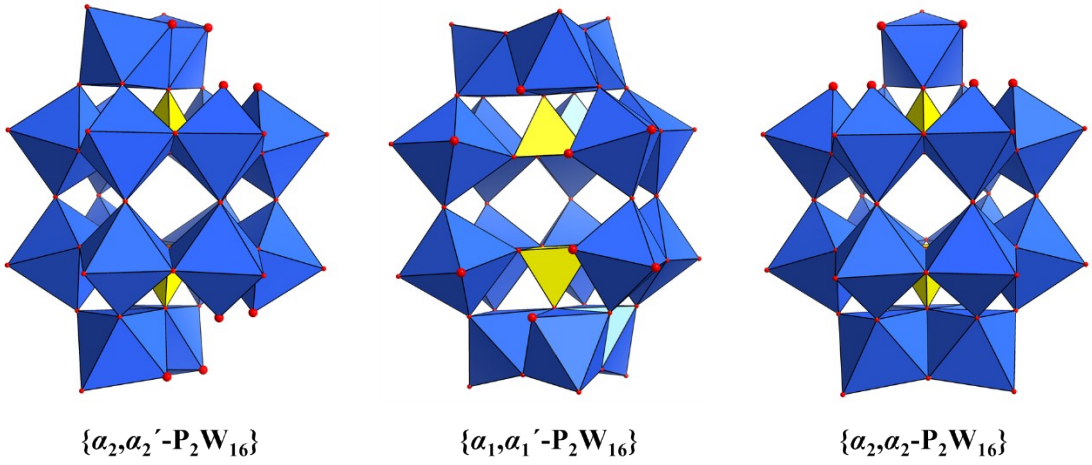

Figure S5. Different isomers of the di-lacunary derivative of Wells-Dawson-type POT, $\{P_2W_{16}\}$, observed $[\alpha_2,\alpha_2'\text{-}P_2W_{16}O_{60}]^{14-}$ ($\{\alpha_2,\alpha_2'\text{-}P_2W_{16}\}$) in this work as well as $[\alpha_1,\alpha_1'\text{-}P_2W_{16}O_{59}]^{12-}$ ($\{\alpha_1,\alpha_1'\text{-}P_2W_{16}\}$) and $[\alpha_2,\alpha_2\text{-}P_2W_{16}O_{59}]^{12-}$ ($\{\alpha_2,\alpha_2\text{-}P_2W_{16}\}$), which was reported in the literature. Color code as in Fig. S2.

FT-IR spectroscopy

Figure S6 shows a comparison of the FT-IR spectra of **D-1** with those of precursor **K-{α_2-P_2W_{17}(PhP)$_2$}**, non-functionalized **K-{α_2-P_2W_{17}}** as well as **CsK-2** based on discrete dimers of the {$Dy_2(\alpha_2,\alpha_2'$-$P_2W_{16})(PhP)_2$} building units featuring a structure similar to **1**. All spectra were recorded in KBr pellets between 4000 and 375 cm^{-1}. The spectrum of **D-1** looks is similar to that of **CsK-2**, in line with the structural affinity of their {$Ln_2(\alpha_2,\alpha_2'$-$P_2W_{16})(PhP)_2$} POM units. It exhibits three bands characteristic for vibrations of P−O bonds of {α_2,α_2'-P_2W_{16}} POT at 1095, 1064 and 1024 cm^{-1} which could be compared with the corresponding bonds at 1097, 1061, and 1026 cm^{-1} in the spectrum of **CsK-2**. As expected, these bands are slightly shifted in comparison with P−O vibrations-associated bands for {α_2-P_2W_{17}}-based samples appearing at 1082, 1049 and 1016 cm^{-1} for **K-{α_2-P_2W_{17}}** and at 1093, 1053 and 1024 cm^{-1} for **K-{α_2-P_2W_{17}(PhP)$_2$}**, that clearly reflects structural rearrangements of the POT skeleton. The shoulders at 1155 and 983 cm^{-1} and a peak at 1133 cm^{-1} in the spectrum of **D-1** could be attributed to the vibrations of P−O and P−C bonds in the phenylphosphonate groups and could be compared with corresponding bands at 1170, 1139 and 985 cm^{-1} and at 1157, 1138 and 976 cm^{-1} in the spectra of **CsK-2** and **K-{α_2-P_2W_{17}(PhP)$_2$}**, respectively.

The intense peak at 941 cm^{-1} in the spectrum of **D-1** reflects stretching vibrations of the terminal W=O bonds and correlates well with the corresponding peaks in the spectra of the **CsK-2** (940 cm^{-1}), **K-{α_2-P_2W_{17}}** (939 cm^{-1}) and **K-{α_2-P_2W_{17}(PhP)$_2$}** (941 cm^{-1}). The bands in the 850 – 400 cm^{-1} range belong to W−O−W, W−O−P and W−O−Ce vibrations. These peaks are similar to those observed in the spectrum of **CsK-2**, while their significant shift with respect to the precursor's peaks further reflects transformation of the POT skeleton upon formation of {$Ln_2(\alpha_2,\alpha_2'$-$P_2W_{16})(PhP)_2$} units in **D-1** (Ln = Ce^{III}) and in **CsK-2** (Ln = Dy^{III}).

The broad band at about 3424 cm^{-1} and the peak at 1626 cm^{-1} are attributed to the stretching and bending vibrations, respectively, of lattice and coordinated water molecules. The series of

peaks ranging from 1612 to 1384 cm^{-1} are caused by stretching and bending vibrations of C=C and C−H bonds in the phenyl rings as well as stretching and bending vibrations of C−N and C−H bonds in the DMA^+ counter cations.

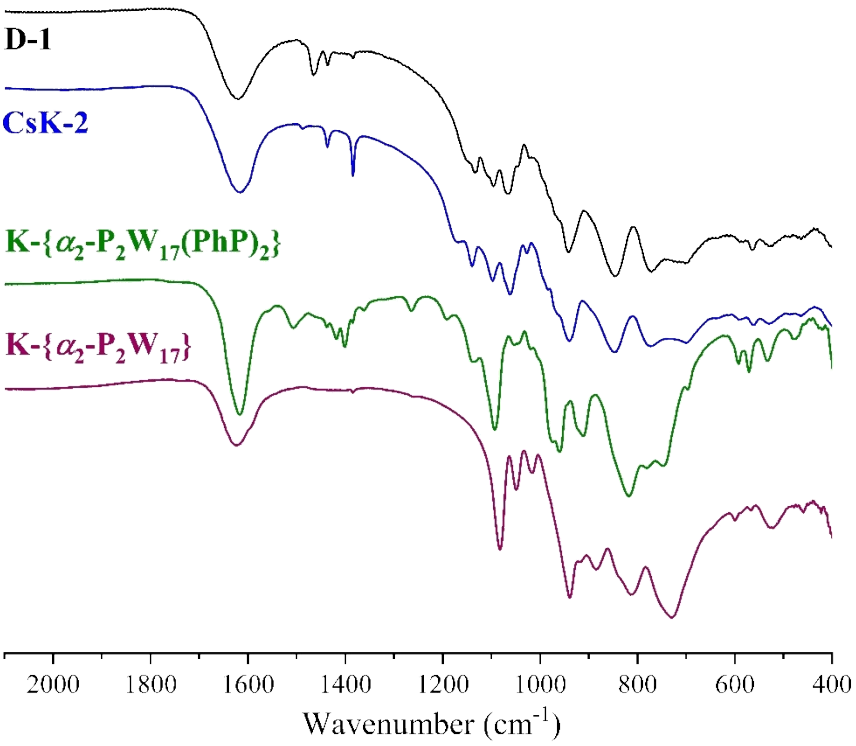

Figure S6. FT-IR spectrum of **D-1** (black line) in comparison to those of **CsK-2** (blue line), **K-{α$_2$-P$_2$W$_{17}$(PhP)$_2$}** (green line) and **K-{α_2-P$_2$W$_{17}$}** (purple line).

Thermogravimetric analysis

The thermal decomposition process for **D-1** was investigated under N_2 atmosphere from room temperature (RT) to 1000 °C (see Figure S7). It occurs in several steps, first of which starts already at RT and is completed at around 250 °C. This decomposition step corresponds to the removal of both 17.5 lattice and coordinated by Ce^{III} ions 8 water molecules per formula unit (calcd. 10.8 *vs.* obs. 9.4 mass %). The slightly smaller than expected (*vs*. the value derived from elemental analysis) water content observed in TGA of **D-1** can be explained by higher degree of dryness of the sample used for the latter study (as is common for polyoxometalate compounds, **D-1** already slowly loses crystal water already at room temperature).

The subsequent weight loss step, occurring in the range from 250 to 600 °C, can be attributed to the release of the dimethylamine cations DMA^+ (most likely via formation of dimethylamine and other decomposition products[7] as well as the combustion of the phenyl groups (calcd. 5.2 *vs.* obs. 4.4 mass %). The processes at temperatures higher than 600 °C belong to the decomposition of the POT skeleton with formation of complex metal oxides.

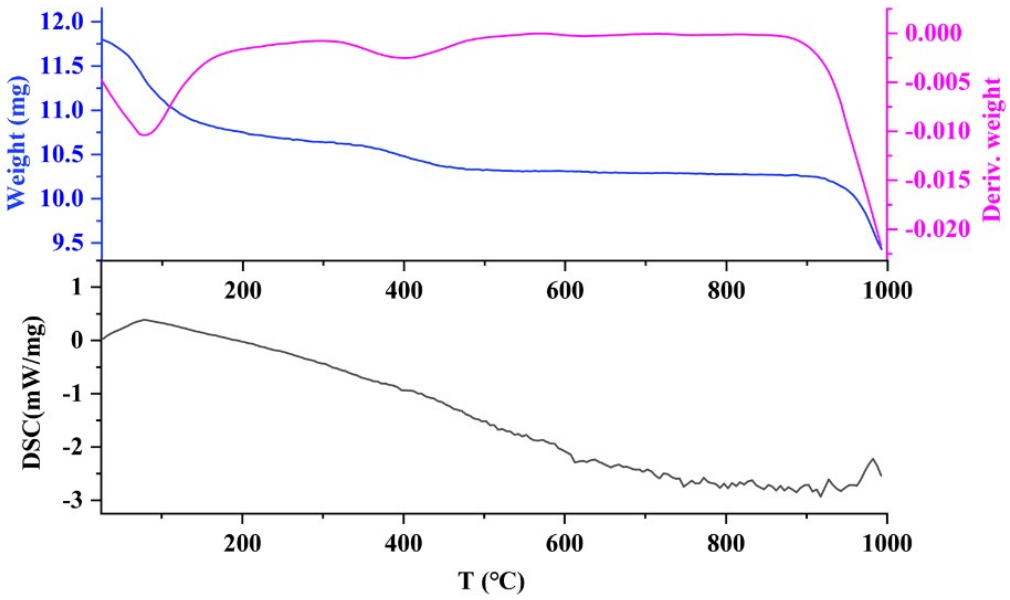

Figure S7. TGA (blue), weight derivative (pink) and SDTA (black) curves for **D-1** from room temperature to 1000 °C under N_2 atmosphere.

Solid-state UV-Vis spectroscopy

Solid-state UV-Vis spectrophotometry of **D-1** was checked to estimate the potential of **D-1** to act as photocatalyst. The obtained spectrum shows a broad light absorption range from 300 to 600 nm (Figure S8) that suggests a broad activation capability by both UV and visible light irradiation. However, preliminary photoelectrocatalytic tests showed only a poor performance of **D-1** for water oxidation.

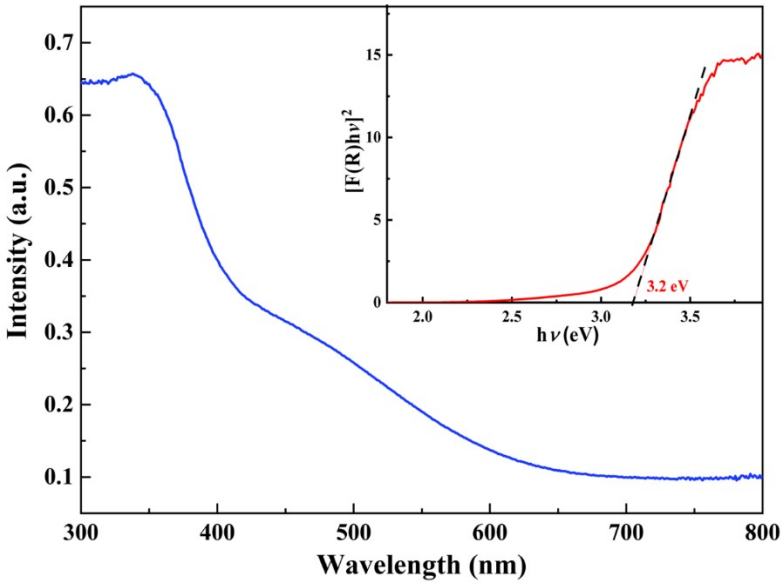

Figure S8. The solid-state UV-Vis absorption spectrum and optical band gap energy (E_g) of (inset) as-prepared **D-1** sample.

References

1. R. Contant, W. G. Klemperer, O. Yaghi, *Inorg. Synth*. 1990, **27**, 104–111.

2. S. Fujimoto, J. M. Cameron, R.-J. Wei, K. Kastner, D. Robinson, V. Sans, G. N. Newton, H. Oshio, *Inorg. Chem.* 2017, **56**, 12169-12177.

3. STOE X-Red32, absorption correction by Gaussian integration, analogous to P. Coppens, The Evaluation of Absorption and Extinction in Single-Crystal Structure Analysis. Crystallographic Computing; F. R. Ahmed, Ed.; Munksgaard: Copenhagen, 1970, pp. 255–270.

4. J. Koziskova, F. Hahn, J. Richter, J. Kožíšek, *Acta Chim. Slov.* 2016, **9**, 136–140.

5. G. M. Sheldrick, *Acta Cryst.* 2015, **C71**, 3–8.

6. H. J. Bunge, *Textures and Microstructures*, 1997, **29**, 1-26.

7. W. K. Musker, *J. Am. Chem. Soc.* 1964, **86**, 960−961.